Collagen packing and mineralization

An x-ray scattering investigation of turkey leg tendon

P. Fratzl,* N. Fratzl-Zelman,‡ K. Klaushofer‡

*Institut für Festkörperphysik der Universität Wien, Strudlhofg.4, A-1090 Wien, Austria; and ‡Ludwig Boltzmann-Institute for Osteology, Fourth Medical Department, Hanusch Hospital, Heinrich-Collin Str. 30, A-1140 Wien, Austria

ABSTRACT Several recent results are suggesting that the collagen packing in mineralized tissues is much less regular than in the case of other nonmineralizing collagen, e.g., rat tail tendon. To clarify this question we have investigated the molecular arrangement in mineralized and unmineralized turkey leg tendon as a model for the collagen of mineralized tissues. Using a combination of diffuse x-ray scattering and computer simulation, it could be shown quantitatively that, although the collagen fibril structure is periodic in the axial direction, it is similar to a two-dimensional fluid in the lateral plane. This has important consequences for the understanding of the mineralization process, which is also discussed.

INTRODUCTION

The mechanical properties of mineralized tissues, like bone, are mainly due to the collagen-mineral interrelationships at molecular level. The structure of bone as composite material is determined by the packing of type I collagen fibrils in which the mineral phase is deposited (1, 2). The axial arrangement of the tropocollagen molecules in the fibrils has been accepted in a virtually unchanged way since the work of Hodge and Petruska (3), but the lateral (equatorial) arrangement is still an unsolved problem. Various models have been proposed, ranging from the packing of microfibrillar substructures (4) or quasihexagonal packing schemes (5, 6) to an arrangement in concentric layers (7). Most of these models assume a regular crystalline arrangement of the molecules, obtained from structure refinements using mainly the x-ray scattering patterns from rat tail tendon (4–6). For wet turkey tendon or demineralized bone collagen, however, it is well known that the x-ray scattering patterns do not consist of sharp Bragg reflexions (as expected for a crystalline structure) but rather of broad, diffuse maxima indicating a much lower degree of order (1, 8). Woodhead-Galloway and Machin (9) have even shown that the x-ray scattering, due to the lateral arrangement of the protocollagen molecules in turkey tendon, is better described assuming a two-dimensional liquid structure rather than a periodic arrangement. Such an interpretation is also supported by growth models for collagen fibrils (10).

Moreover, for mineralized tissues there are some recent observations which are difficult to explain under the assumption of a periodic lateral arrangement of molecules in the collagen fibrils. First, it was found that the Bragg-spacing between the molecules, as deduced from the maximum position of the diffuse x-ray spot, decreases with increasing mineral content (11, 12). Assuming a crystalline arrangement of the molecules in the fibrils, this would imply that (due to lack of space) mineral crystals can not be located within the overlap zone of the fibrils (12), which is in clear contradiction to recent electron microscopic observations (13–16). Secondly, the average thickness of mineral crystals in bone, as determined recently by small-angle x-ray scattering (17, 18), is in the order of 3–4 nm for mice and rats. This is much larger than the typical size of a "hole" ($\approx$1.5 nm [1]) in the gap zone (hole zone) of a collagen fibril. Nevertheless, x-ray data show the presence of such mineral crystals, particularly inside the gap zone (19, 17), but with no trace of lateral order (17, 18).

In order to elucidate these problems, we have reinvestigated the structure of wet, dry and mineralized turkey leg tendon using a quantitative diffuse x-ray scattering method. Turkey leg tendon is, indeed, an ideal model system because tissue with varying degrees of mineralization can be studied on the same sample (13). The calcification of turkey leg tendon has already been studied by electron microscopy (13–16) as well as x-ray scattering (18–20). The only drawback of this system is that the shape of the mineral crystals may not be the same in turkey tendon and in bone (18).

We further use computer simulation to compare quantitatively the measured x-ray spectra to a model which assumes a fluid-like lateral arrangement of molecules in collagen fibrils. This model is shown to account for the observed x-ray scattering patterns and is used to derive a new picture for the collagen-mineral relationship in mineralized tendon and bone.

MATERIALS AND METHODS

Sample preparation

Leg tendons were obtained from 14-wk-old turkeys immediately postmortem. It is well known (13) that these tendons exhibit a strongly mineralized and an unmineralized part with an intermediate region between. The tendons were investigated without further dissection either in the native state or after extensive vacuum drying (3 d in vacuum). In each case, the whole tendon was placed into the x-ray apparatus with the axial collagen direction perpendicular to the incoming x-ray beam. The thickness of the samples was typically a few millimeters in the native state. Measurements were carried out in regions where the tendon was fully mineralized and in others where it was unmineralized. But this provided information only for the native and for the completely dry state of the tendon.

0006-3495/93/01/260/07 $2.00

To investigate the drying procedure in more detail, another procedure has also been used for sample preparation, where it was not necessary to demount the sample between successive measurements (to make sure that always the same region of the sample is covered by the x-ray beam). Immediately after dissection, some tendons were placed into diethylene glycol and treated like in the first step of the water-free embedding method, described, e.g., by Landis et al. (21), without the subsequent polymerization reaction. The glycol is known to replace the water in the sample (21), which was verifyed by measuring the samples immediately after glycol immersion. Indeed, the corresponding x-ray spectra were found similar to the spectra from native tendon. After the glycol treatment, the samples were placed (without container) into the vacuum chamber of the x-ray apparatus and measured continuously for about three days. As glycol is much less volatile than water, the drying process was slow enough to follow it in situ, with a typical time of one hour per spectrum to provide sufficient counting statistics.

X-ray scattering

X-ray scattering experiments were performed using a pinhole camera (with 25 or 100 cm between sample and detector) mounted on a rotating-anode x-ray generator operated with Cu-Kα radiation (wavelength μ = 0.154 nm). The x-ray scattering intensity $I(k)$ was collected as a function of the scattering vector k ($k = 4\pi/\mu \sin(\theta/2)$, where θ is the angle between incident and scattered x-ray beam) using a linear position-sensitive proportional counter.

Hard disk fluid

This model was initially proposed by Woodhead-Galloway and Machin (22) to describe the equatorial structure of collagen (type I) fibrils, and we use their treatment with some modifications. Assuming an undistorted collagen fibril and neglecting the difference between gap and overlap zone, the scattering in the lateral (or equatorial) direction is given by

$$I(k) = I_0 S(k) F(k), \tag{1}$$

where I_0 is a constant (22). $F(k)$ is the equatorial trace of the structure function of a single protocollagen molecule and $S(k)$ describes the correlation in the positions of the molecules in the equatorial plane. In the case of a regular equatorial arrangement on lattice positions, $S(k)$ is zero outside some discrete positions corresponding to the Bragg-reflexions of the lattice. If on the contrary, one assumes a liquid-like arrangement of the molecules in the equatorial plane, $S(k)$ is a continuous function which is non-zero for all k. In particular, approximating the equatorial cross-section of the molecules by a disk of diameter D (corresponding to the smallest possible distance between two molecules) and assuming that the disks can not overlap, one obtains a so-called hard-disk fluid (22–24). This model system has been extensively studied in statistical mechanics and, in particular, the function $S(k)$ is well known. In a good approximation it can be written

$$S(k) = S_{PY}(\phi, kD), \tag{2}$$

where ϕ is the packing fraction of the liquid, i.e.:

$$\phi = w\pi D^2/4, \tag{3}$$

w being the number of molecules by unit surface in the equatorial plane. S_{PY} can be calculated by solving the Percus-Yevick integral equation (24). In this paper, we follow the prescriptions by Woodhead-Galloway and Machin (22) to perform these numerical calculations.

A first estimate for the structure factor $F(k)$ (Eq. 1) of the protocollagen molecule may be obtained in approximating the molecule by a cylinder of diameter D with uniform electron density: this was used in the original model by Woodhead-Galloway and Machin (22). To avoid this unrealistic assumption, we have calculated $F(k)$, taking the atomic positions in the molecule as determined by Fraser et al. (25) and the general formula

$$F(k) = \left\langle \left| \sum_j Z_j \exp(i\mathbf{k}\mathbf{r}_j) \right|^2 \right\rangle, \tag{4}$$

where $\mathbf{r}_j$ means the position of the atom j in projection onto the equatorial plane, $\mathbf{k}$ the scattering vector in this plane and Z_j the number of electrons of the atom j. The brackets denote the circular average. $F(k)$ as calculated by Eq. 4 is compared in Fig. 1 with the structure factor for a homogeneous cylinder.

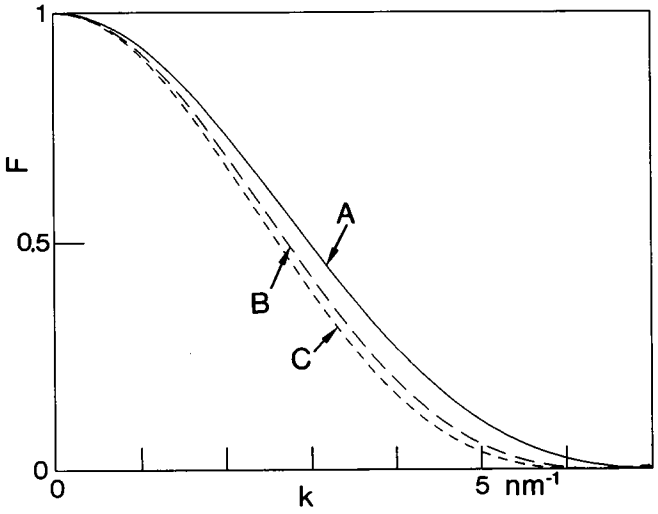

FIGURE 1 Structure factor of a collagen molecule $F(k)$ in projection onto the equatorial plane. The full line (A) shows the calculation using Eq. 4 and the broken lines show in comparison the structure factor approximating the molecule by a homogeneous cylinder with diameter 1.19 nm (B) and 1.23 nm (C). The first value (B) is the effective repulsion diameter found in this study and the second (C) the diameter given by Lees (12).

Taking together Eqs. 2 and 4 and inserting them into Eq. 1, one ends up with an expression for the scattering intensity $I(k)$ depending only on two parameters. The first one is the effective hard disk diameter of the protocollagen molecules (which must be independent of the water content of the fibril) and the second one the packing fraction ϕ, which is a measure for the water content of the fibril.

RESULTS AND DISCUSSION

Lateral packing of collagen

The evolution during the drying process of the equatorial scattering from unmineralized turkey tendon is shown in Fig. 2, *a–d*. Fig. 2 *a* shows the scattering from fresh tendon, and Fig. 2 *b*, *c*, and *d* increasingly dry states. All spectra were recorded using the in-situ drying procedure described earlier (section "sample preparation"). The first feature to be seen in these spectra is that the position k_m of the maximum of $I(k)$ (corresponding to the Bragg spacing d of the molecules, by $d = 2\pi/k_m$) is shifting towards larger values upon drying. This is a commonly observed result (11, 12), and we find that $d \approx$ 1.8 nm for fresh tissue and $d \approx$ 1.1 nm for completely dry tissue, in excellent agreement with earlier studies (11, 12). The second feature, which is frequently over-

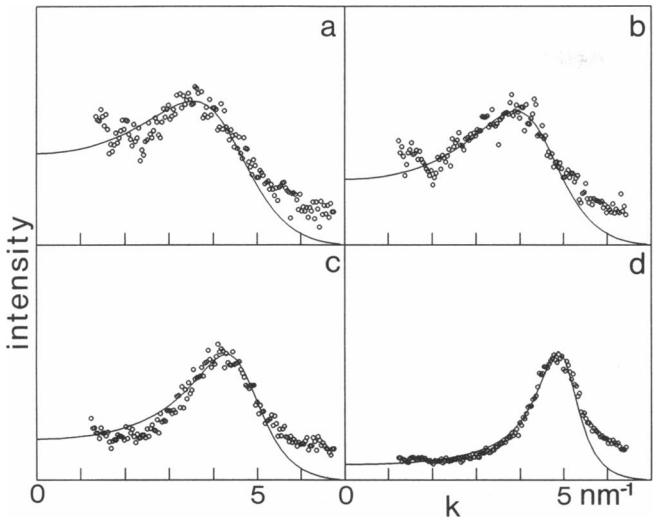

FIGURE 2 Diffuse equatorial x-ray scattering (*circles*) from glycol-treated turkey leg tendon (*a*) and after subsequent vacuum drying for 1 h (*b*), 4 h (*c*), and 17 h (*d*). The full lines correspond to the fit with Eqs. 1–4 (hard disk fluid) with packing fractions of 0.32 (*a*), 0.38 (*b*), 0.46 (*c*), and 0.60 (*d*). The effective repulsion diameter d of the molecules was 1.19 nm in all cases.

looked in the literature, is that the width of the peak changes and not only its maximum position (Fig. 2). Whereas for dry samples the peak is reasonably sharp, it becomes so broad for wet samples that a regular (almost crystalline) arrangement of the molecules becomes completely unlikely. Indeed, if the width of the peak is, in a first approximation, interpreted as the fluctuation of the Bragg-spacings in the tendon, one would have to conclude that the disorder in the molecular spacings increases when the density of molecules decreases. This is a typical property of fluids and, therefore, it might be more appropriate to assume a liquid-like equatorial arrangement, as proposed by Woodhead-Galloway and Machin (22).

Starting from this model, we have performed a quantitative evaluation of our data using the expression for the scattering from a two-dimensional hard-disk fluid (Eqs. 1–4). The molecules are supposed to be distributed at random with the only requirement that they can not overlap. In the resulting expression for $I(k)$, there are only two free parameters. The first one is the packing fraction ϕ (given by Eq. 2) of the molecules in the equatorial plane, and the second one is the hard-disk diameter D of the molecules, which must stay constant during the drying process. We have used expression 1 to fit the data in Fig. 2 (and many similar spectra). The value for D which appeared to be best suited to describe all spectra simultaneously was D = 1.19 nm. This value is of the same order of magnitude as the one determined by Lees (12) from the density of dry tissue (D = 1.23 nm). The small difference between the two diameters is not surprising as their definitions are slightly different, the second one being determined by the mass distribution in the molecule (assumed homogeneous [12]) and the first one by the effective repulsion distance between molecules (see "Hard disk fluid" section).

With the effective diameter D being fixed, the only parameter that varies between the four spectra in Fig. 2 is the packing fraction, which was determined to be $\phi \approx$ 0.32, 0.38, 0.46, and 0.60 for Fig. 2 *a–d*. The functions $I(k)$ obtained from Eq. 1 with these parameters are shown in Fig. 2 by full lines. A good quantitative agreement is found between the data and the model for the variation in the maximum position as well as the width. The small deviation at large k (Fig. 2) could indicate the presence of a background below the data, most probably due to the interfibrillar substance. Another possible explanation could be that the average form factor of the molecules (which was calculated under the assumption of straight molecules) is slightly changed due to distortions of the molecules, which are well known to occur in collagen (1). Nevertheless, the model of lateral fluidity is able to reproduce the essential feature, namely the simultaneous variation in the Bragg-spacings and in the crystallinity (peak width) with water content.

Computer simulation

To further corroborate this result and to obtain pictures of the molecular arrangements, we have generated possible configurations for the molecules in a hard-disk fluid by Monte-Carlo simulation on a computer. The pictures I, II, and III in Fig. 3 *b* show such configurations for three different packing fractions, ϕ = 0.30, 0.56, and 0.70 (the diameter of the black disks is D = 1.19 nm). One can clearly see, that for the higher densities of molecules, there are regions with hexagonal packing appearing in the figure, whereas for the smallest density no such regions can be found. This is in good agreement with the fact that for a packing fraction of $\phi \approx 0.71$, the hard disk fluid freezes to a hexagonal solid (23). With the so generated model samples it is further possible to calculate the x-ray scattering corresponding to each particular configuration, using Eqs. 1 and 4 and the general expression

$$S(k) = \left\langle \left| \sum_n \exp(i\mathbf{k}\mathbf{s}_n) \right|^2 \right\rangle, \qquad (5)$$

where $\mathbf{s}_n$ is the center position of the nth molecule (disk in Fig. 3 *b*) in the equatorial plane. The x-ray scattering, which would be obtained from each of the configurations in Fig. 3 *b*, is shown in the same line in Fig. 3 *c*. The scatter in the data points of Fig. 3 *c* corresponds to statistical fluctuations due to the small size of the model samples (Fig. 3 *b*). These "scattering curves" can be directly compared to real measurements, as shown in Fig. 3 *a*. Sample I corresponds to native unmineralized collagen, II corresponds to slightly dryed collagen (using the glycol-procedure, see "Sample preparation" section), and III to vacuum-dryed collagen (without glycol treatment).

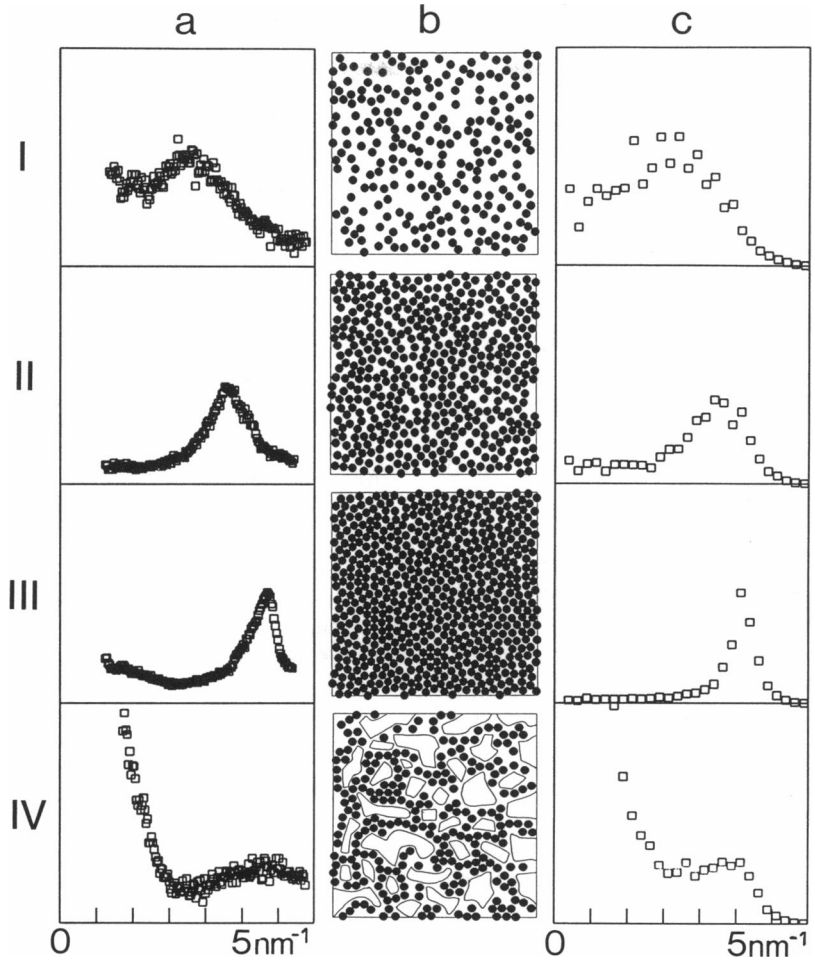

FIGURE 3 (*a*) Diffuse equatorial x-ray spectra measured for fresh (*I*), dehydrated (*II*), and completely dry (*III*) unmineralized turkey leg tendon, as well as for fully mineralized (*IV*) tendon. (*b*) Computer model showing a possible configuration of the hard disk fluid with packing fraction 0.30 (*I*), 0.56 (*II*), and 0.70 (*III*). *IV* contains the same number of molecules (*circles*) as *I*, but they are rearranged to make the place for mineral crystals. (*c*) Diffuse x-ray spectra calculated for the computer samples shown in *b*. In *IV* all space between molecules is supposed to be occupied by mineral.

It is very clear that the "scattering curves" (Fig. 3 *c*) corresponding to the model configurations (Fig. 3 *b*) reproduce all the essential features of the real measurements (Fig. 3 *a*), regarding position and width of the maximum of $I(k)$.

The lines I, II, and III in Fig. 3, therefore, give additional evidence for the fact that the equatorial arrangement of the molecules in wet turkey tendon collagen is rather liquid-like than quasi-hexagonal. Only for dry tendon, the quasi-hexagonal model seems to be a good approximation. Indeed, there are already large regions with fairly well developed hexagonal order in this case (III, in Fig. 3 *b*). Accordingly, the corresponding peak in $I(k)$ is quite sharp (III, in Fig. 3 *c*).

Mineralized collagen

The most important question to be treated now, are the consequences of this observations for the mineralization process. It is well known (11, 12), that the Bragg-spacing of collagen strongly decreases with increasing mineral content. This has led to the conclusion (12) that the crystals must lie between the collagen fibrils and not inside (as far as the overlap zone is concerned). The x-ray scattering curve for dry fully mineralized tendon is shown in Fig. 3 *a* (part IV). We find that the position of the maximum is at quite large values of k, close to the position for dry tendon (III, in Fig. 3 *a*). This is a well known result (20) and it is also known that for wet fully mineralized turkey tendon (with a typical inorganic weight content of 60%) the Bragg-spacing is somewhat larger ($\sim$1.24 nm [20]) but also much smaller than in wet unmineralized tissue. Note, that the strong increase of $I(k)$ towards small k (IV, in Fig. 3 *a*) is due to the small angle scattering (SAXS) from the mineral crystals, which can be used to determine size and orientation of the crystals (17, 18).

In Fig. 3 (part IV), we show that it is possible to imagine a structure for mineralized collagen, where the Bragg-spacing is considerably reduced with respect to wet unmineralized tissue, but where there is still space for mineral deposited inside the overlap zone of the fi-

bril. To interpret the scattering pattern in Fig. 3 *a* (part IV), we start from the picture Fig. 3 *b* (part I), corresponding to native unmineralized collagen. In this liquid-like arrangement there are a number of rather large spaces filled with water, coexisting with regions where the molecules are much closer. Assuming that mineralization starts within the larger spaces and that the crystals grow in thickness until almost all the water is replaced by mineral, one would obtain a situation schematically shown in Fig. 3 *b* (part IV). Here we have assumed that some molecules may be pushed away by the growing crystals until they are touching either another molecule or another crystal. The interesting feature of the structure shown in Fig. 3 *b* (part IV) is that there are regions with a close-packed arrangement of molecules and rather large crystals between. The intermolecular distance in the close-packed regions is close to the value for dry tendon. Accordingly, the calculated scattering function (assuming that all the space between molecules is filled by mineral [IV, in Fig. 3 *c*]) exhibits a maximum at a position very close to the position for dry tendon (III, in Fig. 3 *c*). One also finds the strong increase of $I(k)$ towards small k due to the small angle scattering from the mineral (17, 18). Consequently, the observation of Bragg-spacings which decrease with increasing mineral content does not exclude the existence of crystals within the overlap zone of the collagen! The Bragg-spacing in Fig. 3 *c* (part IV) is the same as for dry tendon, but there is clearly space enough for crystals inside the fibril. The clue for the understanding of this phenomenon is the close-packing of molecules in (very small) regions surrounded by mineral phase (IV, in Fig. 3 *b*).

Moreover, one should emphasize, that these conclusions are true for the overlap zone of the fibril, and even more for the gap zone, because there is larger space for crystals. The model for mineralized tendon (IV, in Fig. 3 *b*) also explains why it is possible to locate crystals with a thickness as large as 4 nm (as found by SAXS [18]) inside the fibril. Depending on the relative speed of crystal formation and crystal growth, it is possible to locate either a larger amount of smaller crystals, or a smaller amount of larger crystals into the fibril without changing its overall volume.

Finally, it is worth to note that the continuous decrease of Bragg-spacing with mineral content as found in bone (11) and in turkey leg tendon (20) can be readily understood within the present model for the mineralization process: In the first stages of mineralization, the mineral is predominantly deposited within the gap-zone of the collagen (as found in earlier studies [1, 2, 16]) and therefore the overlap zone will be almost mineral free. Consequently, the Bragg-spacing in slightly mineralized collagen will be as in mineral-free tissue and drying will lead to a decrease of Bragg-spacing as found experimentally (11, 20). As mineralization goes on, more and more crystals are formed within the overlap zone, pushing

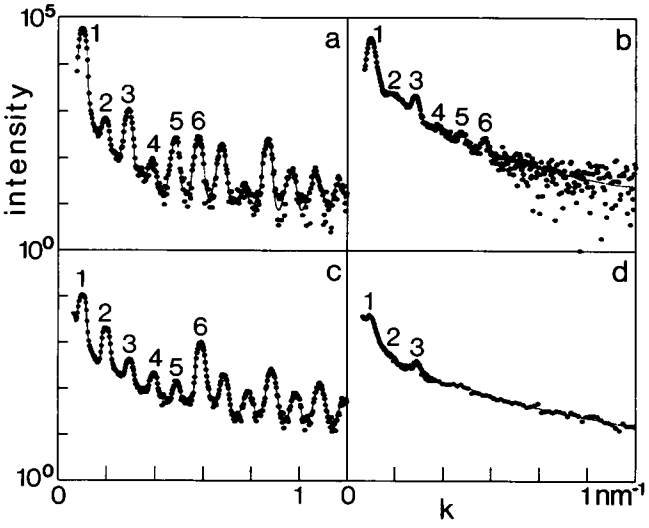

FIGURE 4 Axial x-ray scattering from fresh (*a*) and dry (*c*) unmineralized turkey leg tendon, from fully mineralized turkey leg tendon (*b*) and from the diaphysis of a rat ulna (*d*). The numbers indicate the orders of the axial macroperiod.

away the molecules in the way schematically shown in Fig. 3 (part IV). Therefore, the Bragg-spacing reduces even in wet tissue, as found experimentally (11, 20). When the mineralization process is complete, the Bragg-spacing is reduced to almost the value of dry tissue (11, 20) (see IV, in Fig. 3) and no further reduction of Bragg-spacing upon drying is possible anymore.

Axial packing of collagen

Finally, we show in Fig. 4 the axial (meridional) scattering for (*a*) fresh unmineralized, (*b*) mineralized, and (*c*) vacuum-dryed (unmineralized) turkey tendon, as well as (*d*) cortical bone (rat ulna; the data are taken from reference 17). The conclusions to be drawn from these spectra are mostly well known (19, 17). One observes relatively small second and fourth order peaks for wet collagen (Fig. 4 *a*). This effect, usually ascribed to the electron-density contrast (due to the different water content) between the gap and overlap regions (19), has disappeared in dry tendon (Fig. 4 *c*), probably because the electron density after removal of all water is similar in most parts of the gap and the overlap region.

The peaks corresponding to the collagen macroperiod can also be seen in the case of mineralized tissue (Fig. 4, *b* and *d*), although this signal is now added onto a large scattering background due to the small angle scattering from the mineral crystals (17, 18). In addition, collagen in cortical bone is not arranged in a strictly parallel way as in tendon, the peaks are therefore strongly weakened as can be seen in Fig. 4 *d*. For both dry mineralized tendon (Fig. 4 *b*) and dry cortical bone (Fig. 4 *d*), the second order peak is reduced, like in the case of wet un-

mineralized collagen. Again, this indicates an electron density contrast between gap and overlap regions, most probably related to the fact that mineral is predominantly located in the gap zone (19, 17) of the collagen.

CONCLUSION

The equatorial and meridional x-ray scattering from unmineralized turkey leg tendon collagen has been analyzed quantitatively as a function of the water content and compared with the results for mineralized tendon and bone. It is found that the width of the diffuse peak in the equatorial scattering strongly depends on the water content, which suggests a fluid-like equatorial arrangement of the molecules. Fits of the data using a model of lateral fluidity, proposed as a description for collagen by Woodhead-Galloway and Machin (22), shows that the x-ray data can be reproduced by this model over the whole range of water contents, assuming an effective diameter of 1.19 nm for the protocollagen molecule.

Starting then from a liquid-like arrangement of the molecules in the equatorial plane, a very natural model for the equatorial structure of mineralized collagen is obtained. With the use of computer simulation it could be shown that, just by replacing progressively the water inside the fibril by mineral, it is possible to nucleate reasonably large crystals (as found, e.g., by SAXS [17, 18]) even inside the overlap zone. In some regions of the mineralized tissue (see IV, in Fig. 3 *c*), the protocollagen molecules have then a much smaller spacing than in wet tissue (I, in Fig. 3 *b*), which explains the common observation that the Bragg-spacing of the molecules decreases with the mineral content of the tissue (11, 12). This reconciles the x-ray and neutron scattering data (11, 12) and the electron microscopic observations (1, 2, 12–15) that mineral is first nucleated in the gap zone but continues to extend into the overlap zone at very high degrees of mineralization.

In conclusion, the turkey leg tendon collagen fibrils are extremely regular in the axial direction (as shown by the succession of sharp peaks in Fig. 4), whereas they are quite irregular in the lateral direction, where they are similar to a two-dimensional hard disk fluid. This liquid-crystalline structure is important for the understanding of the mineralization procedure, because it can explain how crystals can be deposited inside the overlap zone of the fibrils, even though the Bragg-spacing between molecules decreases upon mineralization. The shape and thickness of the crystals, which are known to vary for different species (18), may then be controlled by physico-chemical parameters. Indeed, depending on the nucleation rate versus growth rate of the apatite crystals, the tissue could contain either a large number of small crystals or a smaller number of larger crystals. Similarly, the collagen structure would allow the formation of plate-like (as found in turkey leg tendon [18]) as well as needle-like crystals (as found for bone from mice and rats [18]) inside the fibrils.

REFERENCES

1. Veis, A. S., and B. Sabsay. 1987. The collagen of mineralized matrices. *Bone Miner. Res.* 5:1–63.
2. Posner, A. S. 1987. Bone mineral and the mineralization process. *Bone Miner. Res.* 5:65–116.
3. Hodge, A. J., and J. A. Petruska. 1963. Recent studies with the electron microscope on ordered aggregates of the tropocollagen molecule. *In* Aspects of Protein Structure. G. N. Ramachandran, editor. Academic press, New York. 289–300.
4. Trus, B. L., and K. A. Piez. 1980. Compressed microfibril models of the native collagen fibril. *Nature (Lond.).* 286:300–301.
5. Hulmes, D. J. S., and A. Miller. 1979. Quasi-hexagonal molecular packing in collagen fibrils. *Nature (Lond.).* 282:878–880.
6. Lees, S., M. Pineri, and M. Escoubes. 1984. A generalized packing model for type I collagen. *Int. J. Biol. Macromol.* 6:133–136.
7. Parry, D. A. D., and A. S. Craig. 1979. Electron microscope evidence for a 80Å unit in collagen fibrils. *Nature (Lond.).* 282:213–215.
8. Brodsky, B., E. F. Eikenberry, K. C. Belbruno, and K. Sterling. 1982. Variations in collagen fibril structure in tendons. *Biopolymers.* 21:935–951.
9. Woodhead-Galloway, J., and P. A. Machin. 1976. Modern theories of liquids and the diffuse equatorial x-ray scattering from collagen. *Acta Crystallogr.* A32:368–372.
10. Chapman, J. A. 1989. The regulation of size and form in the assembly of collagen fibrils in vivo. *Biopolymers.* 28:1367–1382 and 2201–2205.
11. Lees, S., L. C. Bonar, and H. A. Mook. 1984. A study of dense mineralized tissue by neutron diffraction. *Int. J. Biol. Macromol.* 6:321–326.
12. Lees, S. 1987. Considerations regarding the structure of the mammalian mineralized osteoid from the viewpoint of the generalized packing model. *Conn. Tissue Res.* 16:281–303.
13. Landis, W. J. 1986. A study of calcification in the leg tendons from the domestic turkey. *J. Ultrastruc. Mol. Struct. Res.* 94:217–238.
14. Traub, W., T. Arad, and S. Weiner. 1989. Three-dimensional ordered distribution of crystals in turkey tendon collagen fibers. *Proc. Natl. Acad. Sci. USA.* 86:9822–26.
15. Landis, W. J., J. Moradian-Oldak, and S. Weiner. 1991. Topographic imaging of mineral and collagen in the calcifying turkey tendon. *Conn. Tissue Res.* 25:181–196.
16. Arsenault, A. L. 1991. Image analysis of collagen-associated mineral distribution in cryogenically prepared turkey leg tendons. *Calcif. Tissue Int.* 48:56–62.
17. Fratzl, P., N. Fratzl-Zelman, K. Klaushofer, G. Vogl, K. Koller. 1991. Nucleation and growth of mineral crystals in bone studied by small-angle x-ray scattering. *Calcif. Tissue Int.* 48:407–413.
18. Fratzl, P., M. Groschner, G. Vogl, H. Plenk, Jr., J. Eschberger, N. Fratzl-Zelman, K. Koller, and K. Klaushofer. 1992. Mineral crystals in calcified tissues: a comparative study by SAXS. *J. Bone Miner. Res.* 3:331–336.
19. White, S. W., D. J. S. Hulmes, A. Miller, and P. A. Timmins. 1977. Collagen-mineral axial relationship in calcified turkey leg tendon by x-ray and neutron diffraction. *Nature (Lond.).* 266:421–425.
20. Bigi, A., A. Ripamonti, M. H. J. Koch, and N. Roveri. 1988. Calcified turkey leg tendon as structural model for bone mineralization. *Int. J. Biol. Macromol.* 10:282–286.

21. Landis, W. J., M. C. Paine, and M. J. Glimcher. 1977. Electron microscopic observations of bone tissue prepared anhydrously in organic solvents. *J. Ultrastruct. Res.* 59:1–30.

22. Woodhead-Galloway, J., and P. A. Machin. 1976. X-ray scattering from a gas of uniform hard discs using the Percus-Yevick approximation: an application to a 'planar liquid'. *Mol. Phys.* 32:41–48.

23. Hoover, W. G., and F. R. Ree. 1968. Melting transition and communal entropy for hard spheres. *J. Chem. Phys.* 49:3609–3617.

24. Percus, J. K., and G. J. Yevick. 1958. Analysis of classical statistical mechanics by means of collective coordinates. *Phys. Rev.* 110:1–13.

25. Fraser, R. D. B., T. P. McRae, and E. Suzuki. 1979. Chain conformation in the collagen molecule. *J. Mol. Biol.* 129:463–481.